ISO-LWS Observations of Herbig Ae/Be Stars

D.Lorenzetti

Osservatorio Astronomico di Roma, Monteporzio (Italy)

T.Giannini, B.Nisini, S.Molinari, P.Saraceno, L.Spinoglio

IFSI-CNR Frascati (Italy)

E.Tommasi, S.Pezzuto

ISO Science Operation Centre - Villafranca, Madrid (Spain)

F.Strafella

Università di Lecce (Italy)

P.E.Clegg, G.J.White

Queen Mary & Westfield College - London (UK)

M.Barlow

University College - London (UK)

M.Cohen

Radio Astronomy Laboratory - Berkeley (USA)

R.Liseau

Stockholm Observatory - Saltsjöbaden (Sweden)

F.Palla

Osservatorio Astronomico Arcetri - Firenze (Italy)

H.A.Smith

Harvard-Smithsonian Center for Astrophysics - Cambridge (USA)

Abstract. We present the first results of a survey of Herbig Ae/Be stars (HAEBE) obtained with the Long Wavelength Spectrometer (LWS) on board of ISO. The [OI] and [CII] fine structure lines are the strongest features observed in the 45 - 198 μm range and their intensity ratios are fully compatible with those expected from a photodissociation region. Molecular emission in form of high-J CO rotational transitions is associated with the objects having high density environments and C-shocks mechanism is

293

likely responsible for that. The observed far IR continua have been consistently fitted along with the overall spectral energy distributions (from UV to radio wavelengths). The adopted model computes the continuum emission from star, circumstellar gas and dust arranged in a spherical geometry. A good agreement with the observations is found by adopting dust grains typical of circumstellar environments with an absorption coefficient at FIR wavelengths which follows a dependence shallower than that of standard mixtures.

1. Introduction

So far a great deal of observational work has been done on the HAEBE aiming to clarify their nature and to determine their physical properties and those associated with the close environment. An unbiased picture of this latter is now provided by ISO-LWS spectrophotometry in the far IR (45 - 198μm), a range hitherto unexplored by means of spectroscopic airborne observations, with the exception of HD 200775 (Chokshi et al. 1988). Our targets are listed in Table 1: they constitute a small sample (10 objects), which is nevertheless quite meaningful for exploring a wide range of parameters such as the spectral type (from O7 to A5), the bolometric luminosity (from 30 to 1.3 10^5 L$_\odot$), the circumstellar extinction (from few to more than 10 mag), and the associated outflow activity. In the same table an indication is given for the location of the star and whether or not a close companion has been identified.

Table 1.   Parameters of the observed HAEBE.

Source	SpT	L_{bol} ($L_\odot$)	A_v (*mag*)	Outflow Activity	distance (*pc*)	Companion	Location
LKHα198	B-Ae	340	4.5	CO/HH	600	IR	L1265
V376 Cas	B5	517	5.2	HH	600	opt.	L1265
HD97048	B9.5	30	1.3		150		Cha I
IRAS 12496-7650	A	50	11	CO	250		Cha II
CoD-42°11721	B0	1120	7.1		400		Anon.
R CrA	A5	132	1.9	CO/HH	150	neg.result	NGC 6729
PV Cep	A5	100	0.4-9.5	CO/HH	500		L1158
V645 Cyg	O7	1.3e5	4.9	CO/HH	6000		Anon.
LKHα234	B5/7	283	3.4	CO/HH	1000	IR	NGC 7129
MWC1080	B0	7920	5.3	CO/HH	2500	IR speckle	Anon.

2. Observations

All the HAEBE spectra have been obtained in full grating scan configuration at a resolution R $\sim$ 200, with an instrumental beam size of $\sim$ 80 arcsec; an observation implies a pointing on source and a map of few raster points off source. The criteria we adopted for line detection are quite conservative: *i)* signal to noise ratio S/N $\geq$ 3; *ii)* distance between observed and rest wavelength,

comparable to a small fraction ($\approx$ 25%) of the resolution element ($\approx$ 0.07 and 0.15 μm for short and long wavelength detectors, respectively; *iii)* line width compatible with the nominal value of the relative detector ($\approx$ 0.30 and 0.60 μm).

Details on the observing procedure and data reduction techniques, along with a table containing all the line identifications and relative fluxes are given in Tommasi et al. (this issue).

3. Results and Discussion

3.1. Fine structure lines

The [OI] 63μm and [CII] 158μm fine structure lines are by far the strongest features observed. and are often used, together with [OI] 145μm, as a diagnostic of the excitation mechanism. The observed fluxes are listed in columns 2 to 4 of Table 2 together with their uncertainties. They have obtained by subtraction of the *on* and *off* positions. This procedure does not affect the [OI] lines (which are much stronger on source), but has a definite effect on the [CII] line because of its ubiquity at comparable intensities. In Figure 1a the observed line intensity ratios are reported superimposed on a grid of photodissociation (PDR) models (Luhman et al. 1997). Although the upper limits do not allow a complete derivation of the parameters (G_o, n), the ISO-LWS observations indicate that PDR mechanism can be considered the main excitation source for these lines in HAEBE. In particular we see that the enhancements of the interstellar field (10^2 - 10^4 G_o) are compatible with the spectral types of the stars; moreover indication for relatively high density ($n \geq 10^5 cm^{-3}$) is found for the sources IRAS12496 and RCrA.

Shock models (*e.g.* Hollenbach & McKee 1989) can be ruled out (apart the marginal exception represented by IRAS12496, see Figure 1a) since they predict substantially different line ratios: 20 - 100 and 10 - 10^4 for [OI]63/[OI]145 and [OI]63/[CII]158, respectively. An other argument in favour of a PDR origin is given by the comparison of the mass loss rates derived from published values of the HI recombination and CO lines (columns 5 and 6 of Table 2) and those obtained from the [OI] 63μm line using the relationship given by Hollenbach (1985) (last column of Table 2). Since the values of $\dot{M}$[OI] systematically exceed (by more than one order of magnitude) the other estimates, we can conclude that an additional component of [OI] emission must be the dominant one, such as the PDR emission. As final remark, the obtained spectra indicate how small is the contribution of FIR lines to the IRAS in-band fluxes: the [OI] 63μm line flux is systematically less than 0.2 % of the IRAS 60μm flux, the only exception being represented by CoD-42° 11721, whose relative contribution reaches the value of 0.7 %.

3.2. Molecular lines

In Sec. 3.1 we have given evidence for a high density environment around two sources of our sample. For these sources, where an increased column density is expected, we have also observed CO emission from rotational lines with quantum numbers in the range between J=14 to J=21. In Table 3 the observed transitions

Table 2.   [OI], [CII] line fluxes and derived mass loss rates

Source	[OI] 63μm	[OI] 145μm	[CII] 158μm	M(HI)	M(CO)	M([OI]63μm)
	Flux (10^{-19} Wcm^{-2})				($M_\odot yr^{-1}$)	
LKHα198	2.4 ± 0.8	< 0.7	2.1 ± 0.2	2.0 10^{-7}	3.2 10^{-7}	3.3 10^{-6}
V376 Cas	<0.7	< 0.6	1.9 ± 0.3	-	-	-
HD97048	1.9 ± 0.3	< 0.2	0.6 ± 0.01	-	-	1.7 10^{-7}
IRAS 12496-7650	4.3 ± 0.3	0.31 ± 0.08	< 0.2	-	-	8.8 10^{-7}
CoD-42° 11721	375 ± 5	29 ± 2	125 ± 3	> 5 10^{-7}	-	1.9 10^{-4}
R CrA	56 ± 1	< 3	2.2 ± 1	-	3.3 10^{-7}	3.8 10^{-6}
PV Cep	2.1 ± 0.3	< 0.1	< 0.1	-	5.9 10^{-8}	1.6 10^{-6}
V645 Cyg	7.6 ± 0.8	< 0.6	9.3 ± 0.8	4.5 10^{-7}	1.4 10^{-6}	5.0 10^{-4}
LKHα234	53 ± 1	6.7 ± 0.4	29 ± 0.7	1.4 10^{-7}	4.0 10^{-6}	1.6 10^{-4}
MWC 1080	8.0 ± 0.8	1.2 ± 0.4	4.0 ± 0.4	3.1 10^{-6}	3.1 10^{-6}	2.0 10^{-4}

for IRAS12496 are indicated, the results for RCrA are reported in Giannini et al. (this issue), together with a detailed investigation of whole region. CO transitions have been observed for the source LKHα234 as well (Tommasi et al. this issue). Fits to the data points are obtained using an LVG code (Nisini et al. this issue) and are shown in their figure 1. Despite its simplified treatment of the geometry of the source and of radiative transfer, this code allows the possible ranges of the temperature and density to be determined. The resulting relatively high densities ($n \sim 10^6 cm^{-3}$) obtained for the considered sources indicate that the CO emitting region is not too different from that where PDR emission originates.

Table 3.   Observed CO line intensities of the source IRAS12496-7650

λ (obs.) (μm)	Line ident.	Flux (10^{-20} Wcm^{-2})	S/N
123.99	J (21 →20)	<3.1	-
130.42	J (20 →19)	1.4	2.8
137.13	J (19 →18)	2.7	5.4
144.71	J (18 →17)	4.2	8.4
153.32	J (17 →16)	5.4	9.0
162.84	J (16 →15)	4.6	9.2
173.62	J (15 →14)	3.6	7.2
186.00	J (14 →13)	<6.0	-

In order to identify the excitation mechanism for the CO lines, the luminosity ratio of neutral Oxygen and CO is reported in Figure 1b as a function of ie density, for different G$_o$, adopting the PDR models by Burton, Hollenbach : Tielens (1990) (open circles), and for different shock velocity, adopting the C-iock model by Draine, Roberge & Dalgarno (1983) (filled circles). The observed ita for RCrA, LKHα234 and IRAS12496 are reported as dashed horizontal bars hich indicate the measured luminosity ratios *vs* the range of densities derived
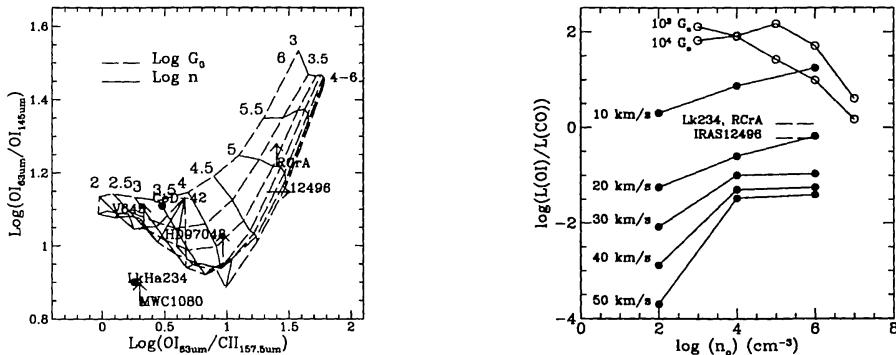
Figure 1.   a) Observed line ratios superposed to PDR models. b) Neutral Oxygen and CO luminosity *vs* density: comparison between observations and models (PDR and C-shocks)

from LVG model (10^5 - 10^6 cm^{-3}); these data, superposed to the model predictions, suggest that non-dissociative C-shock is more likely the mechanism responsible for molecular excitation.

3.3.   Model fits to the continua

ISO-LWS spectrophotometry is the unique mean for providing spectral energy distributions (SED's) at wavelengths and spectral resolution unexplored by IRAS. We have obtained fits to the observed continua by using a spherical model which is characterized by a central object along with a typical ionization structure: an HII region and a region where metals are photoionized. The dust is delimited by its sublimation temperature and can overlap the metal region (Berrilli et al. 1992; Pezzuto, Strafella & Lorenzetti 1997). Four radiative processes are considered (free-free, free-bound, electron scattering and dust emission), and the absorption coefficients k_ν are computed as a function of the radial coordinate, once the density and temperature law are given. A circumstellar-type extinction coefficient (*i.e.* corresponding to dust particles having mean sizes greater than those of the interstellar medium) has been used, with a shallow dependence on wavelength ($\lambda^{-0.8}$ or $\lambda^{-1.2}$) in the far IR. By using such a model we obtain satisfactory fits of the observed SED's (see Figure 2) over a wide range of wavelengths (from U to radio band), indicating that a spherical model is quite appropriate for the majority of the HAEBE in our sample (six out of ten). In Figure 2 the crosses in the (sub)millimetric range indicate the values computed by diffracting the model fluxes according to the telescope beam used in the corresponding observation. The last panel shows an enlargement of the LWS portion for CoD-42°11721 where observations and model are indicated by solid and dashed lines, respectively; the IRAS data (crosses) coincide, within the errors, with ISO-LWS spectrophotometry. Finally the reliability of our model has been checked *a posteriori*, by looking at the agreement between the literature
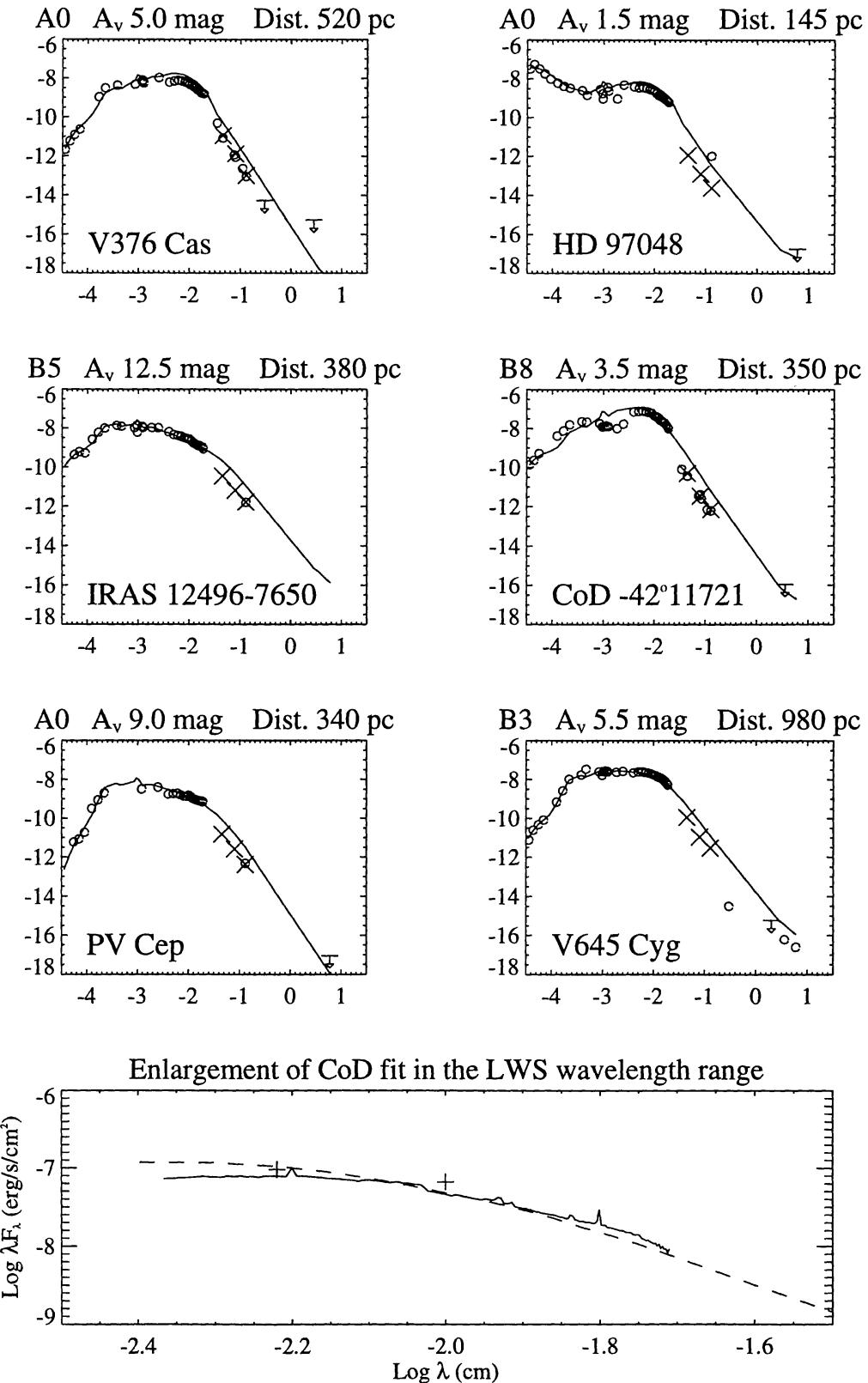
Figure 2.   Best fits to the observed SED's

data for spectral type, extinction and distance and the values relative to our model which are reported in the individual panels of Fig.2.

References

Berrilli, F., Corciulo, G., Ingrosso, G., Lorenzetti, D., Nisini, B., & Strafella, F. 1992, ApJ, 398, 254

Burton, M.G., Hollenbach, D. & Tielens, A.G.G.M. 1990, ApJ, 365, 620

Chokshi, A., Tielens, A.G.G.M., Werner, M.W., & Castelaz, M.W. 1988, ApJ, 334, 803

Draine, B.T., Roberge, W.G., & Dalgarno A. 1983, ApJ, 264, 485

Hollenbach, D. 1985, Icarus, 61, 36

Hollenbach, D., & Mc Kee, C.F. 1989, ApJ, 342, 306

Luhman, M.L., Jaffe, D.T., Sternberg, A., Herrmann, F., & Poglitsch, A. 1997, ApJ, 482, 298

Pezzuto, S., Strafella, F., & Lorenzetti, D. 1997, ApJ, in press

Part 8

Poster papers